Murine Coronaviruses Encoding nsp2 at Different Genomic Loci Have Altered Replication, Protein Expression, and Localization[▽]

Mark J. Gadlage,[2,3] Rachel L. Graham,[1,3]† and Mark R. Denison[1,2,3]*

Departments of Pediatrics[1] and Microbiology and Immunology[2] and The Elizabeth B. Lamb Center for Pediatric Research,[3] Vanderbilt University Medical Center, Nashville, Tennessee

Partial or complete deletion of several coronavirus nonstructural proteins (nsps), including open reading frame 1a (ORF1a)-encoded nsp2, results in viable mutant proteins with specific replication defects. It is not known whether expression of nsps from alternate locations in the genome can complement replication defects. In this report, we show that the murine hepatitis virus nsp2 sequence was tolerated in ORF1b with an in-frame insertion between nsp13 and nsp14 and in place of ORF4. Alternate encoding or duplication of the nsp2 gene sequence resulted in differences in nsp2 expression, processing, and localization, was neutral or detrimental to replication, and did not complement an ORF1a Δnsp2 replication defect. The results suggest that wild-type genomic organization and expression of nsps are required for optimal replication.

Coronaviruses are positive-sense RNA viruses that translate the first open reading frames (ORFs; ORF1a and ORF1b) of their 30-kb genome RNA into polyproteins that are co- and posttranslationally processed into intermediate and mature nonstructural proteins (nsps; nsps 1 to 16). The nsps interact on cytoplasmic membranes at sites of viral RNA synthesis, referred to as replication complexes (4, 5, 10, 17, 22, 25). Translation of ORF1b, which encodes several proteins confirmed or predicted to be essential for viral RNA synthesis, requires a ribosomal frameshift event at the end of ORF1a that occurs at 10 to 40% efficiency in vitro (2, 9, 13–15, 18, 21, 23).

The murine hepatitis virus (MHV) nsp2 is a 65-kDa protein that has minimal sequence identity or similarity among different coronavirus groups and has no known or predicted functions. We have shown for MHV and severe acute respiratory syndrome coronavirus (SARS-CoV) that in-frame deletion of nsp2 (Δnsp2) yields viable mutant viruses (12). However, both MHV and SARS-CoV Δnsp2 mutants exhibit a 90% reduction in peak titer and a 50% reduction in viral RNA synthesis. To determine if expression of nsp2 from nonnative sites could complement the defect in MHV Δnsp2 replication, we engineered the nsp2 coding sequence at alternate sites in the genome both in the absence and in the presence of the wild-type ORF1a nsp2 sequence. The results indicate that nsp2 can be encoded and expressed alone from ORF4, as a sequence duplication in ORF1a and ORF1b or in ORF1a and ORF4, but not near the end of ORF1a or alone in ORF1b. Duplication or expression of the nsp2 sequence from ORF4 was detrimental to replication compared to that of the wild type, indicating that the native context of nsp2 expression, and possibly a single copy of the sequence, may be necessary for optimal function in

replication. Results also indicate that the addition of amino acids at the N and C termini of natively expressed nsp2 has no effect on peak viral growth.

nsp2 can be encoded in replication-competent mutant viruses in ORF4 and between nsp13 and nsp14 in ORF1b. MHV nonessential ORFs have been shown to tolerate foreign gene insertion (3, 8, 19). In order to test the effects of nsp2 expression in downstream ORFs, we engineered a mutant MHV genome by substitution of the nsp2 coding sequence in place of the nonessential ORF4 coding sequence, while retaining the ORF4 transcriptional regulatory sequence (5′-CUAAAC-3′) and start codon (Fig. 1 and Table 1). To determine if nsp2 could be expressed from alternate locations in the replicase, we engineered the nsp2 sequence at the end of ORF1a following nsp10 (nsp10-11 and nsp10-12 junction) and in ORF1b between nsp13 and nsp14. Since processing between nsp10-12 and nsp13-14 is mediated by nsp5 (3CLpro), we designed minimal 3CLpro recognition cleavage sites of P2-LeuGln ↓ Ser-P1′ (16, 20, 27) at the amino and carboxyl termini of nsp2 by the addition of a Ser residue to the N terminus of nsp2 and LeuGln residues to its C terminus, leaving the 3CLpro recognition sequences of nsp10, nsp12, nsp13, and nsp14 intact. The wild-type N-terminal nsp2 residue is Val; we selected Ser as a conservative addition that would optimize for cleavage by nsp5. We have previously shown that P1′ substitutions at the amino terminus of nsp2 that allow processing (Ala, His) do not affect virus growth or RNA synthesis (6); however, to determine if Ser and LeuGln additions had any effects on nsp2 functions of alternately expressed nsp2 viruses, these mutations were engineered into natively expressed nsp2 in a wild-type virus background.

Infectious viruses with the following mutations were recovered from supernatants of electroporated cells: ORF4 deletion, with or without ORF1a nsp2 expression (1a-2/Δ4 and Δ1a-2/Δ4); ORF4 nsp2 with or without ORF1a nsp2 expression (1a-2/4-2 and Δ1a-2/4-2); ORF1b nsp2 with ORF1a nsp2 expression (1a-2/13-2-14); and ORF1a nsp2 with amino acid additions at the N and/or C terminus (1a-S2, 1a-2LQ, and 1a-S2LQ). The supernatants from electroporated cells were passed to expand the populations (pas-
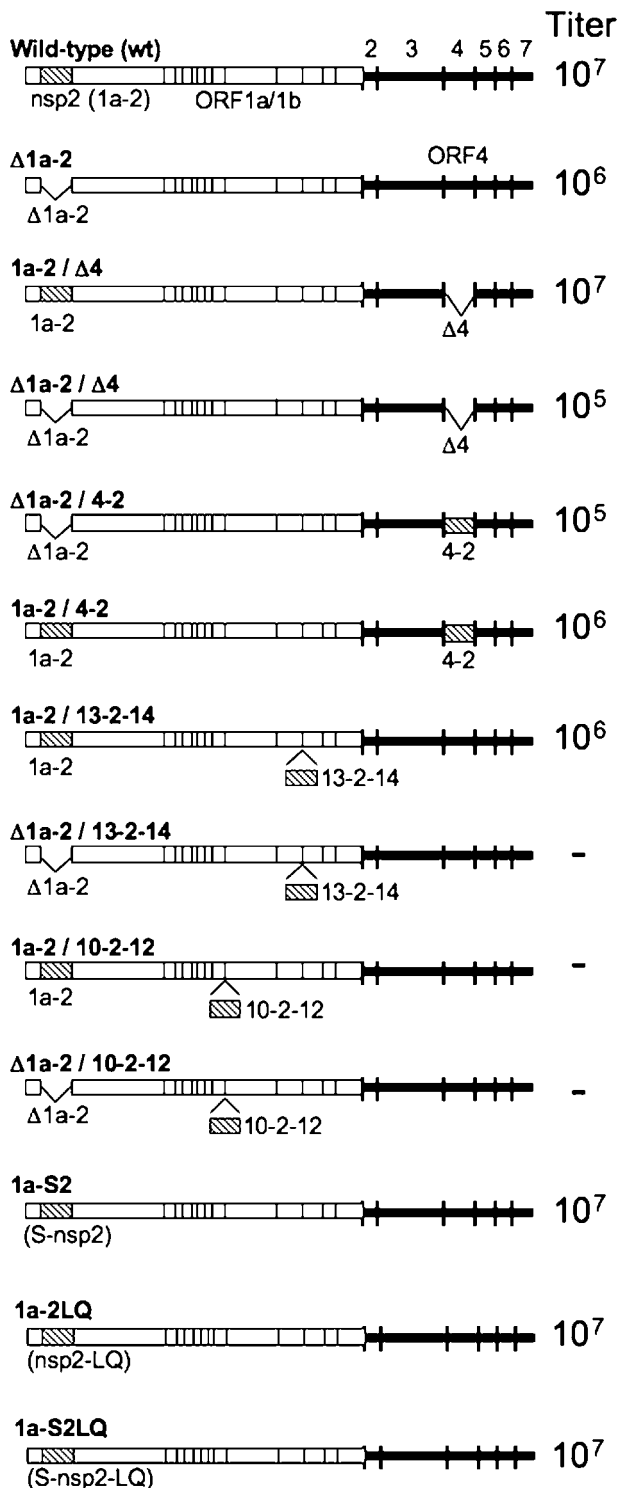
FIG. 1. Engineering nsp2 deletions, mutations, rearrangements, and duplications. For each construct, alterations to the genome are shown. Constructs are listed as named in the text. ORFs 1 to 7 are labeled above the wild-type schematic. The nsp2 coding sequence is depicted as a hatched rectangle. Coding region locations and sizes are not drawn to scale. Deletion of the nsp2 and/or ORF4 coding sequence or insertion of nsp2 in ORF1b is indicated by a caret. Protein coding deletions are indicated by a delta (Δ) in the virus name. The nsp2 position is indicated as ORF1a (1a-2), ORF1b (13-2-14 or 10-2-12), or ORF4 (4-2). Approximate peak titers of viable viruses are indicated to

sage 1 [P1]), and RNA from cells infected with P1 virus stocks was used to confirm the retention of all engineered changes from recovered mutants. Multiple attempts to recover mutants lacking ORF1a nsp2 but expressing nsp2 in ORF1b (Δ1a-2/13-2-14) failed to produce infectious virus. We also were not able to recover mutants encoding nsp2 in-frame between nsp10 and nsp12, with or without ORF1a nsp2 expression (1a-2/10-2-12 and Δ1a-2/10-2-12).

Protein expression and processing from nsp2 alternate expression and duplication viruses. To determine the expression and processing of nsp2 in mutant virus infections, lysates of radiolabeled, virus-infected DBT cells were immunoprecipitated with antisera against nsp1, nsp2, and nsp3 (Fig. 2A). Mature nsp1 (28 kDa) was detected in all mutant virus-infected cells, demonstrating normal processing between nsp1 and nsp2 by the nsp3 papain-like proteinase 1 (PLP1). Mutant viruses that expressed nsp2 from ORF1a (1a-2/Δ4, 1a-2/13-2-14, and 1a-2/4-2) and the Δnsp2 virus (Δ1a-2) all produced similar amounts of nsp1 relative to that of the wild type, while the Δ1a-2/Δ4 and Δ1a-2/4-2 viruses expressed lower levels of nsp1. nsp3 was detectable with anti-nsp3 in wild-type-infected cells as both mature nsp3 (210 kDa) and intermediate nsp2-3 (275 kDa). Mutant viruses that encoded nsp2 in its native position (1a-2/Δ4, 1a-2/4-2, and 1a-2/13-2-14) also had detectable nsp3 and nsp2-3. Only mature nsp3 was detected in infections with viruses that lacked ORF1a-expressed nsp2 (Δ1a-2, Δ1a-2/Δ4, and Δ1a-2/4-2).

As expected, mutant viruses that did not encode nsp2 at any location (Δ1a-2 and Δ1a-2/Δ4) had no detectable nsp2. Viruses encoding nsp2 from one or two locations in the genome exhibited a range of nsp2 expression levels. The Δ1a-2/4-2 virus expressed low levels of nsp2, while the 1a-2/Δ4 mutant virus expressed nsp2 at levels similar to those expressed by the wild type. The 1a-2/4-2 duplication mutant, which encoded nsp2 in both ORF1a and ORF4, expressed higher levels of nsp2 than the wild-type virus. To test whether the increased expression was due to just two coding locations or if there were also altered levels of ORF4 subgenomic RNA, infected cells were labeled with [^{3}H]uridine in the presence of actinomycin D, and viral RNAs were measured by densitometry by using ImageJ 1.40 (http://rsb.info.nih.gov/ij/) (Fig. 2B). All genomic and subgenomic RNA species were detected, but RNA4 encoding nsp2 in ORF4 in the 1a-2/4-2 virus was expressed with a 2.5-fold increase, as a ratio to RNA7, compared to wild-type virus. This is sufficient to account for the increased nsp2 levels and suggests that insertion of foreign genes in ORF4 may specifically alter mRNA transcription.

The 1a-2/13-2-14 mutant virus, which encoded nsp2 in both ORF1a and ORF1b, expressed overall levels of mature nsp2 that were comparable to those expressed by the wild type. This could have resulted from either diminished translation from ORF1b or impaired or absent processing. The requirement for in-frame translation of nsp13 and nsp14 for virus viability argues that the in-frame nsp2 must be translated from this loca-

the right of each construct. Viruses that were not recovered are indicated by a minus sign (−).

TABLE 1. Description of primers

Primer	Sequence	Sense	Purpose
nsp13-nsp2 A	5′GTCAATGACACCACTCGCAAGTATGTGTTTACT	+	PCR partner for nsp13-nsp2 B
nsp13-nsp2 B	5′CGTCTCGCACACTGTAATCGTGGATTGTTAATCTT	−	Insertion mutagenesis partner for A
nsp2 1b Ins C	5′CGTCTCGTGTGTTAAGCCCATCCTGTTTGTGGAC	+	nsp2 ORF1b insertion mutagenesis
nsp2 1b Ins D	5′CGTCTCGCTGTAATCGCGCACAGGGAAACCTCCAGCACTG	−	nsp2 ORF1b insertion mutagenesis
nsp2-nsp14 E	5′CGTCTCGACAGTGTACTACAAATTTGTTTAAGGATTGT	+	Insertion mutagenesis partner for F
nsp2-nsp14 F	5′CATGTGAGCTCAAAGCTGGCAGCCCACGTCAC	−	PCR partner for nsp2-nsp14 E
ORF4 Ins A	5′CAGGCCATAGAAAAGGTCAATGAGTGCGTT	+	PCR partner for ORF4 Ins B primers
ORF4 Ins2 B1	5′CGTCTCGCCATCTATAAATTGTTTAGATTTTCTG	−	Insertion mutagenesis partner for A
ORF4 InsKo B2	5′CGTCTCGTTTATTACTATAAATTGTTTAGATTTTCTG	−	ORF4 deletion partner for A
ORF4 nsp2 C	5′CGTCTCGATGGTTAAGCCCATCCTGTTTGTGGAC	+	nsp2 ORF4 insertion mutagenesis
ORF4 nsp2 D	5′CGTCTCGTTTATTACGCACAGGGAAACCTCCAGCACTG	−	nsp2 ORF4 insertion mutagenesis
ORF4 Ins E	5′CGTCTCGTAAACTCCAAGAGGTTTTGATTATAGTACA	+	Insertion mutagenesis partner for F
ORF4 Ins F	5′CTTAAGGAATTGAACTGCCTCGTCGGCCGT	−	PCR partner for ORF4 Ins E
S-nsp2 F	5′GGGCTATCGCGGTTCTGTTAAGCCCATCCTG	+	Insertion mutagenesis partner for S-nsp2 R
S-nsp2 R	5′CAGGATGGGCTTAACAGAACCGCGATAGCCC	−	Insertion mutagenesis partner for S-nsp2 F
nsp2-LQ F	5′GGTTTCCCTGTGCGCTCCAAGGCAAGAAAGTCGAG	+	Insertion mutagenesis partner for nsp2-LQ R
nsp2-LQ R	5′CTCGACTTTCTTGCCTTGGAGCGCACAGGGAAACC	−	Insertion mutagenesis partner for nsp2-LQ F
158 A F	5′TCCGGCTCGTATGTTGTGTGGAAT	+	PCR partner for S-nsp2 R and nsp2-LQ R
3253 A R	5′CTGCGTCAAGCACAACATCAAGCA	−	PCR partner for S-nsp2 F and nsp2-LQ F

tion in ORF1b. The efficiency of ribosomal frameshifting and translation of ORF1b relative to ORF1a has not been experimentally tested during virus infection but is predicted to be less than 25% (2). This would be consistent with the detection of minimal additional nsp2. The lack of detection would also result if expressed nsp2 was not cleaved from nsp13 or nsp14, or both and thus was not detected as mature nsp2. Immunoprecipitation with anti-nsp2 or anti-nsp13 antisera did not resolve precursors consistent with a predicted size for nsp13-2 (130 kDa), nsp2-14 (130 kDa), or nsp13-2-14 (190 kDa) (data not shown). Taken together, these data indicate that the level of protein expression depends on a combination of the number of coding sequence copies and the context of expression.

Localization of nsp2 in cells during infection with mutant viruses. To determine if nsp2 localization was affected by genomic location and extent of expression, DBT cells were infected, and at 6 h postinfection (p.i.), cells were fixed and stained with antibodies against nsp2 and nsp8, both markers for replication complexes (1) (Fig. 3). nsp2 and nsp8 signals colocalized in characteristic cytoplasmic perinuclear foci in cells infected with viruses expressing both nsp2 and nsp8 (wild type, 1a-2/Δ4, and Δ1a-2/4-2). When expression of nsp2 was absent (Δ1a-2/Δ4), no nsp2 signal was present, while nsp8 signal was still detected in punctate foci. nsp2 expressed from the 1a-2/4-2 virus showed partial colocalization with nsp8 signal, but nsp2 was also detected as diffuse cytoplasmic fluorescence that was not associated with punctate foci. A possible explanation for this result is that simultaneous expression of nsp2 from ORF1 and ORF4 in the 1a-2/4-2 virus saturates replication complexes. This would be consistent with the observed increase in nsp2 expression (Fig. 2A). This conclusion is also supported by the observation that infection with the 1a-2/13-2-14 mutant, which resulted in lower levels of mature nsp2 (Fig. 2A), showed colocalization of nsp2 with nsp8, but no additional localization or diffuse fluorescence (Fig. 3). While direct proof of differential localization of nsp2 would require unique tags for nsp2 at different loci, it is still clear that alteration of nsp2 coding location within the genome results in differences in both extent of protein expression and localization of nsp2 during infection.

nsp2 encoded at different loci results in varied effects on viral growth but does not complement nsp2 deletion from ORF1a. To assess the effects of alternate nsp2 encoding on viral replication, DBT cells were infected at a multiplicity of infection (MOI) of 1 PFU/cell, aliquots of supernatant were saved, and titers of virus were determined by a plaque assay (Fig. 4). As has been shown previously (8), the deletion of ORF4 resulted in a mutant virus that had growth kinetics and peak titers indistinguishable from those of the wild type (Fig. 4A). Deletion of nsp2 alone (Δ1a-2) resulted in a decrease of ~1 $\log_{10}$ compared to the wild type, also consistent with previous studies (11). Expression of nsp2 from ORF4 in the presence or absence of ORF1a nsp2 was similar to that of the parental Δ1a-2 mutant in the timing of exponential growth. However, the 1a-2/4-2 virus reached a slightly higher titer than the Δ1a-2 virus but did not achieve wild-type growth at 24 h p.i. (Fig. 4B), suggesting that expression of nsp2 at increased total levels may in fact be detrimental to virus growth fitness. Also, the Δ1a-2/4-2 virus achieved a 0.5-$\log_{10}$ lower peak titer than the Δ1a-2 virus, and the titer declined more rapidly than that of either the Δ1a-2 or the 1a-2/4-2 virus over a 24-h period. The results show that ORF4 expression of nsp2 does not complement the deletion of nsp2 from ORF1a and suggest that ORF4 expression of nsp2 in the absence of ORF1a nsp2 expression results in a less-fit mutant virus. When nsp2 was expressed in ORF1b (1a-2/13-2-14), growth was delayed in timing, and peak titer could not reach that of the wild-type virus at 24 h p.i., even though peak titers were still increasing, similarly to the 1a-2/4-2 virus (Fig. 4B).

We were surprised that the deletion of both nsp2 and ORF4 or nsp2 replacement of ORF4 (Δ1a-2/Δ4 and Δ1a-2/4-2) yielded mutants with more delayed and/or decreased growth than deletion of either nsp2 or ORF4 alone (Fig. 4A). These results suggest possible interactions and/or cooperative functions of nsp2 and the ORF4 protein(s) in the viral life cycle. Both nsp2 and the ORF4 gene product(s) are group-specific proteins (7, 17, 28) and may have as-yet-uncharacterized interactions. Alternatively, it is possible that the known replication defect of the Δnsp2 mutant exacerbates a replication defect in an ORF4 deletion mutant that alone does not manifest as a
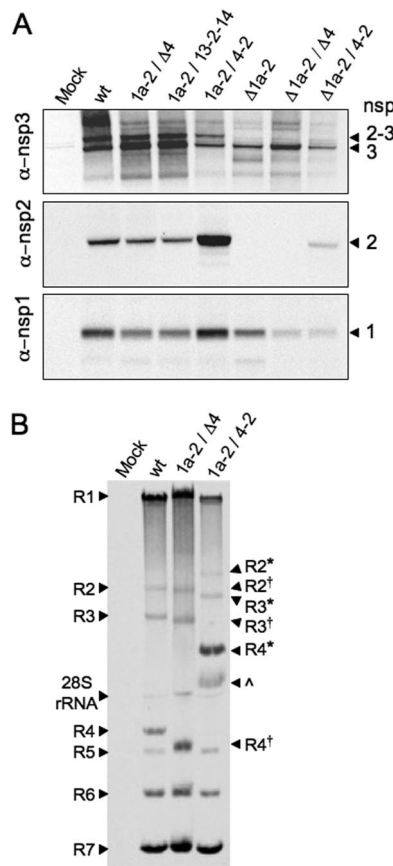
FIG. 2. Protein expression, processing, and RNA synthesis of altered nsp2 viruses. DBT cells were infected with viruses as indicated above the gels. (A) Proteins were radiolabeled, and cell lysates were immunoprecipitated with anti-nsp1, anti-nsp2, and anti-nsp3 antibodies. "Mock" indicates mock-infected cells and "wt" indicates recombinant wild-type MHV-A59. nsps are indicated to the right of the gel: nsp2-3 (275 kDa), nsp3 (210 kDa), nsp2 (65 kDa), and nsp1 (28 kDa). (B) Viral RNA was metabolically labeled with [³H]uridine in the presence of actinomycin D from 9 to 11 h p.i. Intracellular RNA was isolated, denatured, and resolved by electrophoresis. Genomic RNA (R1) and subgenomic mRNAs (R2 to R7) are indicated. R2, R3, and R4 from the 1a-2/Δ4 virus are approximately 300 bp shorter than wild-type mRNAs and are indicated by a superscript †. The 1a-2/Δ4 virus was used as a control in which ORF4 is deleted, but its transcriptional regulatory sequence is still present, resulting in R4 comigrating with R5. R2, R3, and R4 from the 1a-2/4-2 virus, which are approximately 1,400 bp longer than wild-type R2, R3, and R4, are indicated with ∗. An unknown band, possibly an R4 degradation product, is indicated by a caret. R1 from wild-type and mutant viruses exhibited some variability in migration. This variability is supported by quantification of overall genomic RNA levels (1a-2/Δ4 > wt > 1a-2/4-2). RNA band sizes and quantification were determined by using ImageJ 1.40. α, anti.

change in growth kinetics in culture. Finally, it is possible that altered RNA folding or protein-RNA interactions resulting from the cumulative deletion of >2 kb of genome is responsible for the observed replication defect and decrease in expression of nsps 1 to 3. This possibility is supported by the result that 1a-2/4-2 virus had a slight growth delay, grew to peak titers of >1 log₁₀ higher than those of Δ1a-2/Δ4, and exhibited higher expression levels of nsps 1 to 3.

Additions of amino acids at the N and/or C terminus of nsp2 do not affect peak viral growth. Because alternately expressed nsp2 was engineered to contain minimal 3CLpro cleavage sites
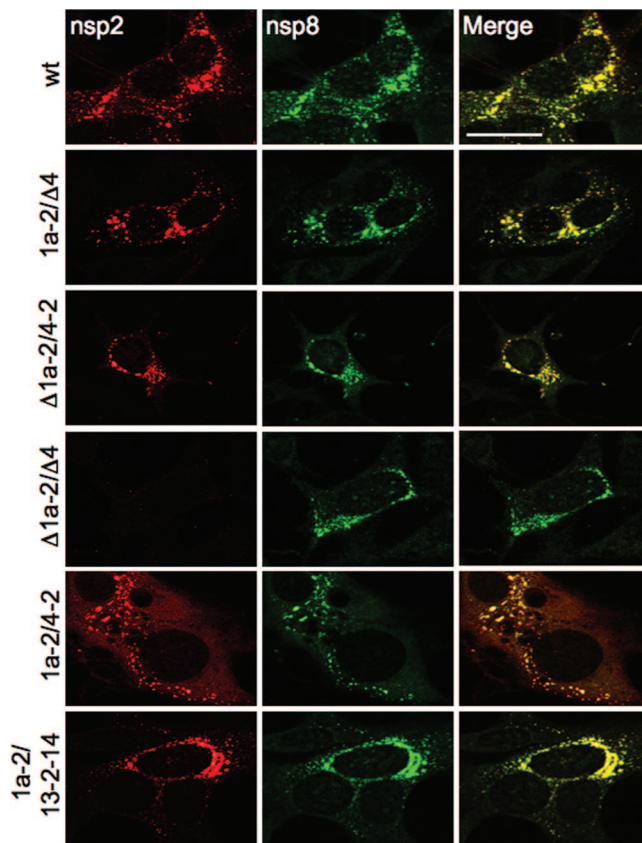

FIG. 3. Immunofluorescence of nsp2 mutants. DBT cells on glass coverslips were infected for 6 h, fixed, and stained for nsp2 and nsp8 by Alexa546 conjugated to a secondary immunoglobulin G (IgG) antibody and by Alexa488 directly conjugated to a primary IgG antibody, respectively. Colocalization is indicated by yellow pixels in the merged images. The bar in the upper right image equals 20 μm and is representative for all images. Images were obtained on a Zeiss LSM510 and were processed in Adobe Photoshop CS2.

(P2-LeuGln ↓ Ser-P1′) when introduced between nsp13 and nsp14 to promote cleavage, we next wanted to determine the effects of introducing amino acids at the N and C termini of nsp2 on viral growth. Therefore, viruses were engineered to have an addition of a Ser residue at the N terminus (1a-S2), LeuGln residues at the C terminus (1a-2LQ), or both mutations (1a-S2LQ) in the native location of nsp2 (Fig. 1 and Table 1). Viral growth experiments were performed as previously described at an MOI of 0.1 PFU/cell, and the 1a-S2, 1a-2LQ, and 1a-S2LQ viruses reached peak growth similar to that of wild-type virus (Fig. 5A), suggesting that the additional amino acids do not inhibit functions of nsp2 in cell culture. However, the 1a-2LQ and 1a-S2LQ viruses were slightly delayed in exponential growth compared to wild-type virus. Protein processing experiments show detection of mature nsp2 in the 1a-2LQ and 1a-S2LQ viruses (Fig. 5B), yet pulse-chase analysis reveals decreased expression of mature nsp2 in the 1a-2LQ and 1a-S2LQ viruses compared to wild-type virus (Fig. 5C). These observations are consistent with the previously described ΔCS2 mutant virus, which has a delay in exponential growth, can reach peak titers similar to those of wild-type virus, and exhibits no mature nsp2 detection (Fig. 5A and B). There-
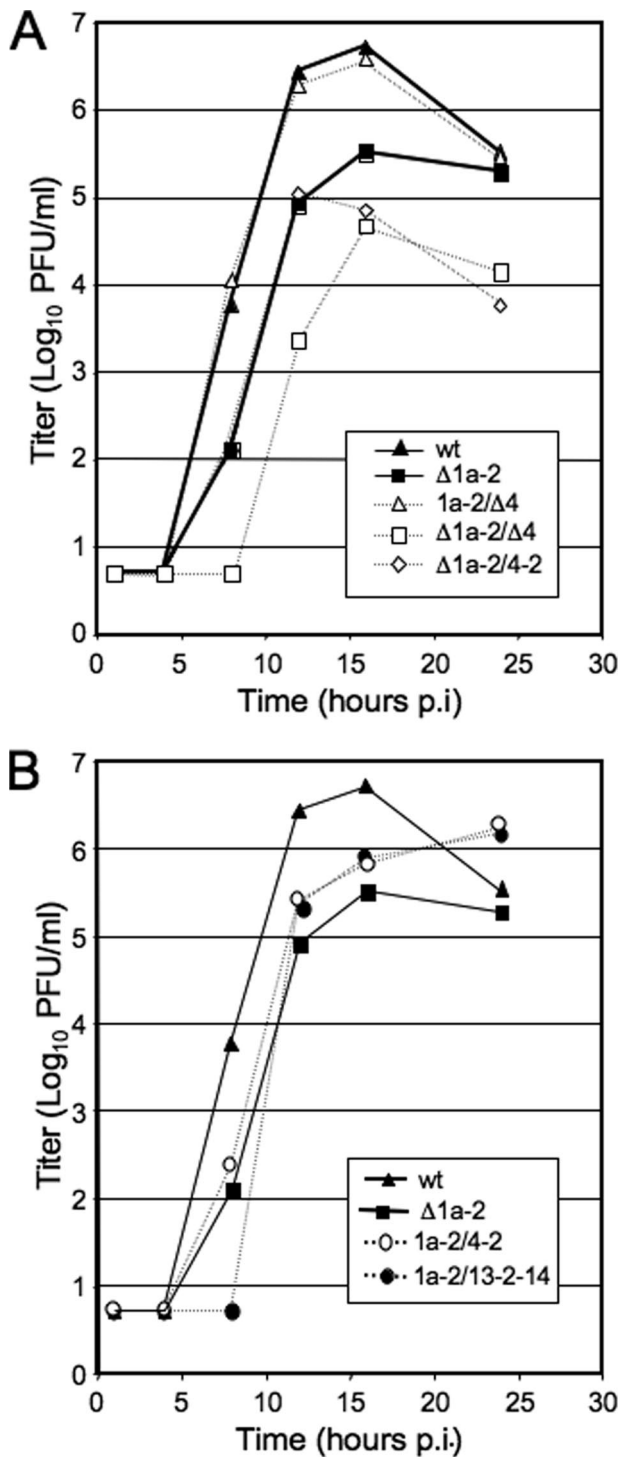
FIG. 4. Growth of nsp2 alternate expression viruses. DBT cells were infected with indicated viruses at an MOI of 1 PFU per cell. Aliquots of supernatant were taken at indicated times p.i., and titers were determined by a plaque assay. All infections were performed in the same experiment with replicates. (A) nsp2 and ORF4 deletion and ORF4 single expression mutants. (B) nsp2 duplication viruses. Wild-type curve and Δ1a-2 curve from panel A are duplicated in panel B to allow direct comparison.
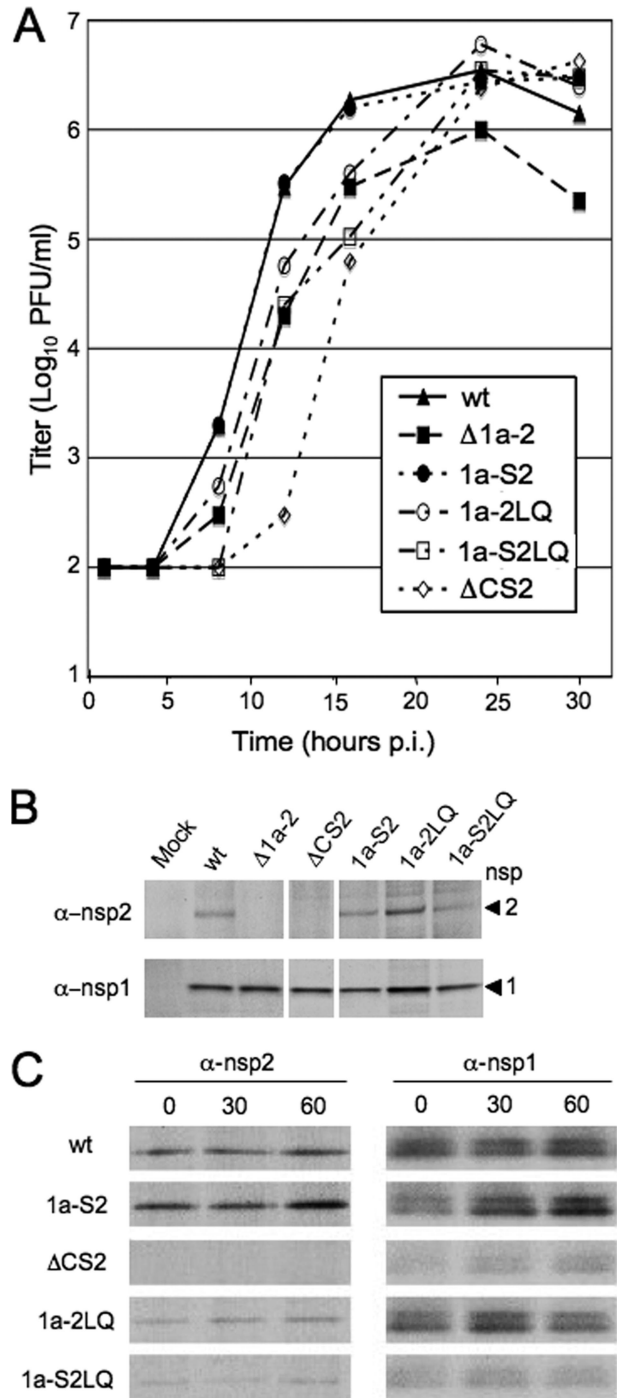
FIG. 5. Growth and protein processing of 1a-S2, 1a-2LQ, and 1a-S2LQ viruses. (A) DBT cells were infected with indicated viruses at an MOI of 0.1 PFU/cell. Viral titers were determined as described in the text. Infections were performed in the same experiment with replicates. (B) Protein processing experiments were performed as previously described. Immunoprecipitations were performed with anti-nsp1 and anti-nsp2 antibodies. All samples were resolved on the same gel, but the image was cropped to remove extraneous lanes. (C) Pulse-chase analysis was performed by infecting DBT cells at an MOI of 10 PFU/cell. Proteins were radiolabeled, and cell lysates were immunoprecipitated with anti-nsp1 and anti-nsp2 antibodies. The presence of an nsp1 doublet has been previously described and may be due to alternative cleavage or posttranslational modifications of nsp1 (24). Viruses are indicated to the left of the gels, and the time of chase (in minutes) is indicated at the top of the gels. α, anti.

fore, the additions of amino acids at the N and C termini of nsp2 appear to affect processing and not the overall functions of nsp2.

The results of this study demonstrate that it is possible for nsp2 to be encoded from alternate locations in the genome, either alone or in combination with ORF1a nsp2, and that alternate location or expression results in a range of effects on growth, expression, RNA synthesis, and localization. Of interest, it was recently reported that an nsp2-EGFP fusion protein could be expressed from the nonessential MHV ORF2b (26). Although the replication phenotype of this virus was not reported, the result is consistent with our study and indicates that additional sites of nsp2 expression/duplication are tolerated. In our experiments, the modest growth defect of an nsp2 deletion is not complemented by expression from ORF1b or ORF4, suggesting that whatever function nsp2 serves, the timing and/or interactions resulting from expression between nsp1 and nsp3 are likely critical for its role. Specifically, it is known that nsp2 is detectable as an nsp2-3 intermediate and that abolition of processing of nsp2 from nsp3 results in a prolonged eclipse phase, while abolition of processing between nsp1 and nsp2 results in diminished growth (6, 11). This was consistent with our observation that the addition of amino acids to the N terminus had no effect on processing and had wild-type growth, while the addition of residues to the C terminus of nsp2 altered processing and eclipse phase, but not peak viral growth. Thus, the results suggest that nsp2 may serve as an important *cis* regulatory protein for nsp1 and nsp3.

Since nsp2 is dispensable for replication, the results here cannot directly predict the rearrangement effects of essential replication proteins, such as nsp5 (3CLpro) and nsp12 (RNA-dependent RNA polymerase). However, our results have shown that additional protein sequence can be encoded not only in the downstream ORFs but also in the replicase between nsp13 and nsp14, suggesting flexibility in both ORF1a and ORF1b for deletion, introduction, and reordering of protein domains. Demonstration that an ORF1 protein can be expressed from alternate locations and can still target to replication complexes suggests that it will be possible to test the effects of alteration of location and extent of expression of critical replication proteins on virus viability, growth, and pathogenesis.

REFERENCES

1. **Bost, A. G., E. Prentice, and M. R. Denison.** 2001. Mouse hepatitis virus replicase protein complexes are translocated to sites of M protein accumulation in the ERGIC at late times of infection. Virology **285:**21–29.
2. **Brierley, I., P. Digard, and S. C. Inglis.** 1989. Characterization of an efficient coronavirus ribosomal framshift signal: requirement for an RNA pseudoknot. Cell **57:**537–547.
3. **de Haan, C. A., B. J. Haijema, D. Boss, F. W. Heuts, and P. J. Rottier.** 2005. Coronaviruses as vectors: stability of foreign gene expression. J. Virol. **79:**12742–12751.
4. **Denison, M. R., A. C. Sims, C. A. Gibson, and X. T. Lu.** 1998. Processing of the MHV-A59 gene 1 polyprotein by the 3C-like proteinase. Adv. Exp. Med. Biol. **440:**121–127.
5. **Denison, M. R., W. J. Spaan, Y. van der Meer, C. A. Gibson, A. C. Sims, E. Prentice, and X. T. Lu.** 1999. The putative helicase of the coronavirus mouse hepatitis virus is processed from the replicase gene polyprotein and localizes in complexes that are active in viral RNA synthesis. J. Virol. **73:**6862–6871.
6. **Denison, M. R., B. Yount, S. M. Brockway, R. L. Graham, A. C. Sims, X. Lu, and R. S. Baric.** 2004. Cleavage between replicase proteins p28 and p65 of mouse hepatitis virus is not required for virus replication. J. Virol. **78:**5957–5965.
7. **de Vries, A. A. F., M. C. Horzinek, P. J. M. Rottier, and R. J. deGroot.** 1997. The genome organization of the nidovirales: similarities and differenced between arteri-, toro, and coronaviruses. Semin. Virol. **8:**33–47.
8. **Fischer, F., C. F. Stegen, C. A. Koetzner, and P. S. Masters.** 1997. Analysis of a recombinant mouse hepatitis virus expressing a foreign gene reveals a novel aspect of coronavirus transcription. J. Virol. **71:**5148–5160.
9. **Gorbalenya, A. E., E. V. Koonin, A. P. Donchenko, and V. M. Blinov.** 1989. Coronavirus genome: prediction of putative functional domains in the nonstructural polyprotein by comparative amino acid sequence analysis. Nucleic Acids Res. **17:**4847–4861.
10. **Gosert, R., A. Kanjanahaluethai, D. Egger, K. Bienz, and S. C. Baker.** 2002. RNA replication of mouse hepatitis virus takes place at double-membrane vesicles. J. Virol. **76:**3697–3708.
11. **Graham, R. L., and M. R. Denison.** 2006. Replication of murine hepatitis virus is regulated by papain-like proteinase 1 processing of nonstructural proteins 1, 2, and 3. J. Virol. **80:**11610–11620.
12. **Graham, R. L., A. C. Sims, S. M. Brockway, R. S. Baric, and M. R. Denison.** 2005. The nsp2 replicase proteins of murine hepatitis virus and severe acute respiratory syndrome coronavirus are dispensable for viral replication. J. Virol. **79:**13399–13411.
13. **Ivanov, K. A., T. Hertzig, M. Rozanov, S. Bayer, V. Thiel, A. E. Gorbalenya, and J. Ziebuhr.** 2004. Major genetic marker of nidoviruses encodes a replicative endoribonuclease. Proc. Natl. Acad. Sci. USA **101:**12694–12699.
14. **Ivanov, K. A., V. Thiel, J. C. Dobbe, Y. van der Meer, E. J. Snijder, and J. Ziebuhr.** 2004. Multiple enzymatic activities associated with severe acute respiratory syndrome coronavirus helicase. J. Virol. **78:**5619–5632.
15. **Koonin, E. V.** 1991. The phylogeny of RNA-dependent RNA polymerases of positive-strand RNA viruses. J. Gen. Virol. **72:**2197–2206.
16. **Lu, X. T., A. C. Sims, and M. R. Denison.** 1998. Mouse hepatitis virus 3C-like protease cleaves a 22-kilodalton protein from the open reading frame 1a polyprotein in virus-infected cells and in vitro. J. Virol. **72:**2265–2271.
17. **Masters, P. S.** 2006. The molecular biology of coronaviruses. Adv. Virus Res. **66:**193–292.
18. **Minskaia, E., T. Hertzig, A. E. Gorbalenya, V. Campanacci, C. Cambillau, B. Canard, and J. Ziebuhr.** 2006. Discovery of an RNA virus 3′->5′ exoribonuclease that is critically involved in coronavirus RNA synthesis. Proc. Natl. Acad. Sci. USA **103:**5108–5113.
19. **Oostra, M., E. G. te Lintelo, M. Deijs, M. H. Verheije, P. J. Rottier, and C. A. de Haan.** 2007. Localization and membrane topology of coronavirus nonstructural protein 4: involvement of the early secretory pathway in replication. J. Virol. **81:**12323–12336.
20. **Piñón, J. D., H. Teng, and S. R. Weiss.** 1999. Further requirements for cleavage by the murine coronavirus 3C-like proteinase: identification of a cleavage site within ORF1b. Virology **263:**471–484.
21. **Ricagno, S., M. P. Egloff, R. Ulferts, B. Coutard, D. Nurizzo, V. Campanacci, C. Cambillau, J. Ziebuhr, and B. Canard.** 2006. Crystal structure and mechanistic determinants of SARS coronavirus nonstructural protein 15 define an endoribonuclease family. Proc. Natl. Acad. Sci. USA **103:**11892–11897.
22. **Schiller, J., A. Kanjanahaluethai, and S. C. Baker.** 1998. Processing of the coronavirus mhv-jhm polymerase polyprotein: identification of precursors and proteolytic products spanning 400 kilodaltons of ORF1a. Virology **242:**288–302.
23. **Snijder, E. J., P. J. Bredenbeek, J. C. Dobbe, V. Thiel, J. Ziebuhr, L. L. Poon, Y. Guan, M. Rozanov, W. J. Spaan, and A. E. Gorbalenya.** 2003. Unique and conserved features of genome and proteome of SARS-coronavirus, an early split-off from the coronavirus group 2 lineage. J. Mol. Biol. **331:**991–1004.
24. **Sparks, J. S., E. F. Donaldson, X. Lu, R. S. Baric, and M. R. Denison.** 2008. A novel mutation in murine hepatitis virus nsp5, the viral 3C-like proteinase, causes temperature-sensitive defects in viral growth and protein processing. J. Virol. **82:**5999–6008.
25. **van der Meer, Y., E. J. Snijder, J. C. Dobbe, S. Schleich, M. R. Denison, W. J. Spaan, and J. K. Locker.** 1999. Localization of mouse hepatitis virus nonstructural proteins and RNA synthesis indicates a role for late endosomes in viral replication. J. Virol. **73:**7641–7657.
26. **Verheije, M. H., M. Raaben, M. Mari, E. G. Te Lintelo, F. Reggiori, F. J. van Kuppeveld, P. J. Rottier, and C. A. de Haan.** 2008. Mouse hepatitis coronavirus RNA replication depends on GBF1-mediated ARF1 activation. PLoS Pathog. **4:**e1000088.
27. **Ziebuhr, J., and S. G. Siddell.** 1999. Processing of the human coronavirus 229E replicase polyproteins by the virus-encoded 3C-like proteinase: identification of proteolytic products and cleavage sites common to pp1a and pp1ab. J. Virol. **73:**177–185.
28. **Ziebuhr, J., V. Thiel, and A. E. Gorbalenya.** 2001. The autocatalytic release of a putative RNA virus transcription factor from its polyprotein precursor involves two paralogous papain-like proteases that cleave the same peptide bond. J. Biol. Chem. **276:**33220–33232.